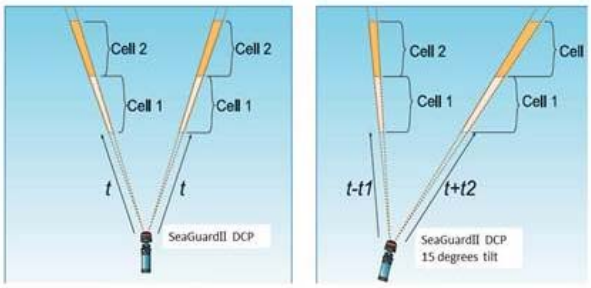

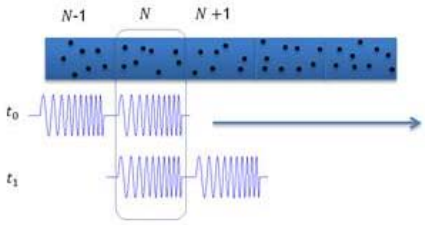

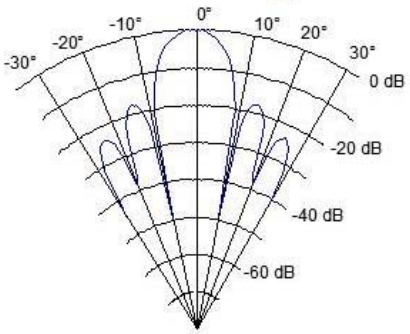

DCPS Theoretical Primer

AANDERAA
a xylem brand

Preliminary Edition 16th December 2015

TABLE OF CONTENT

Introduction

Purpose and scope

This manual gives a basic and simplified theoretical background to the measurement principles of Acoustic Doppler Current Profilers with focus on the Aanderaa Doppler Current Profiling Sensor (DCPS 5400/5402/5403).

CHAPTER 1 The Doppler principle

This chapter gives a basic description of the Doppler principle and how it could be used to measure relative radial velocity between different objects.

1.1 The Doppler effect

Acoustic Doppler Current Profilers measure water velocity using a principle of physics discovered by Christian Johann Doppler (1842). The Doppler effect relates to the change in frequency for an observer moving relative to a source of sound or light. Doppler first stated his principle in the article, '*Concerning the coloured light of double stars and some other constellations in the heavens*'.

In daily life a common example of the Acoustic Doppler effect or Doppler shift is the siren of an ambulance as it approaches, passes and recedes from an observer. Compared to the emitted frequency, the received frequency is higher during the approach, identical at the instant of passing by, and lower during recession. When the source of the waves is moving towards the observer, each successive wave crest is emitted from a position closer to the observer than the previous wave. Therefore, each wave takes slightly less time to reach the observer than the previous wave. Hence, the time between the arrival of successive wave crests at the observer is reduced, causing an increase in the frequency (compressed sound waves). Conversely, if the source of waves is moving away from the observer, each wave is emitted from a position farther from the observer than the previous wave, so the arrival time between successive waves is increased, reducing the frequency. The distance between successive wave fronts is then increased (stretched out sound waves). The total Doppler effect result therefore from motion of the source and motion of the observer.

The relationship between the source frequency, f_s and the Doppler shifted frequency, f_D, can be given by:

$$f_D = f_s\left(\frac{c+v_o}{c-v_s}\right) \qquad \textbf{Eq. 1}$$

Where c is the speed of sound, v_o is the velocity of the observer and v_s is the velocity of the source.

In terms of the corresponding periods equation 1 becomes:

$$T_D = T_s\left(\frac{c-v_s}{c+v_o}\right) = T_s\frac{f_S}{f_D} \qquad \textbf{Eq. 2}$$

1.2 Doppler shifts using acoustic scatterers

A Doppler current profiler applies the Doppler principle by acting both as source and receiver while bouncing short pulses of acoustic energy off particles/scatterers (e.g. clay, silt, bubbles, phytoplankton, zooplankton) that are always present in natural waters. The scatterers are floating in the water and are assumed to move with the same horizontal and vertical speed as the water. The scatterers will reflect the transmitted sound energy back in all directions and a small amount of the reflected signal is Doppler shifted towards the receiver. Because the instrument both transmits and receives sound pulse, the Doppler shift is doubled (once on the way to the scatterers and a second time on the way back after reflection). Assuming that the velocity of the particles (v_0) and the instrument/source (v_s) are much slower than the speed of sound ($v_O << c$ and $v_s << c$), the resulting equation for the Doppler shift becomes:

$$\Delta f = 2 f_S \frac{v_O}{c} \qquad \textbf{Eq. 3}$$

Example:
With a 600 kHz transmitted sound frequency, 1500m/s speed of sound and scatterers moving at 1 cm/s, the Doppler shift is:

$$\Delta f = 2 \cdot 600e^3 Hz \frac{0.01 \ m/s}{1500 \ m/s} = 8 \ Hz$$

But what we explained so far only works when sound sources and receivers get closer to or further from one another.

1.3 Decomposition of Doppler shift / radial motion

If we come back to the ambulance approaching the observer directly, the pitch would remain constant until the vehicle hit him, and then immediately jump to a new lower pitch. Because the vehicle passes by the observer, the radial velocity does not remain constant, but instead varies as a function of the angle between his line of sight and the ambulance's velocity.

In the **figure 1-1** a transmitter transmits a signal towards a reflector (scatterer). In the first figure the reflector is stationary. The circles around it indicates the wavelength of the returned signal in all directions; for a stationary target the wavelength of reflected signal will be the same in all directions and it will have the same frequency as transmitted, and no Doppler shift regardless of the angle.

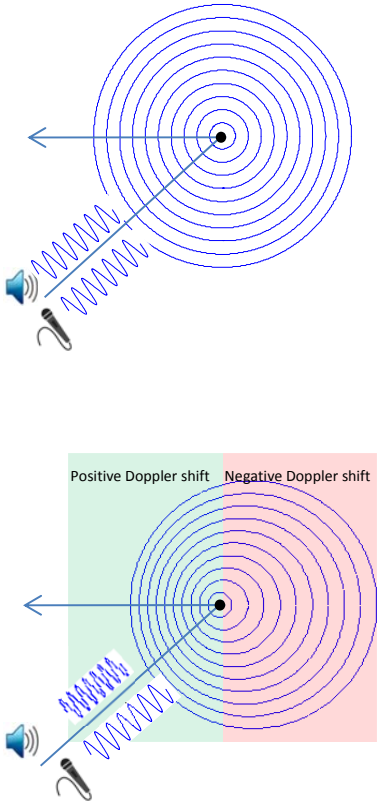

Figure1-1: Doppler shift from a stationary and moving target

For a moving reflector as in the second figure, the wavelength/frequency of the reflected signal will differ depending on the position of the receiver. The Doppler shift will depend on both the target speed and the angle θ between the direction of the moving target, and the direction from the target to the transmitter. We assume that the source is stationary. For angles θ <90° the Doppler shift is positive and for angles θ >90°, the Doppler shift is negative.

At θ =90° there is no Doppler shift. The angular motion changes the direction between the source and the receiver but not the distance separating them.

The derived Doppler shift as function of speed and direction can be then expressed as:

$$f_d = f_s \left(\frac{c+v_s}{c-v_s} \right) \cdot \cos(\theta) \quad \textbf{Eq. 4}$$

CHAPTER 2 Narrowband / Broadband – principles of operation

2.1 Geometry and features of the Aanderaa Doppler Current Profiling Sensor

The Aanderaa Doppler Current Profiling Sensor (DCPS) has four transducers acting both as transmitters and receivers. All four transducers transmit acoustic pulses simultaneously at approximately 600kHz. The transducers are oriented 90° in azimuth from each other and with a 25° angle to the vertical.

They are incorporated into a cylindrical shaped housing that contains all the necessary electronics offering an independently working sensor. It includes a three axis solid state compass able to obtain the current direction independently of the sensor orientation and to constantly measure and compensate the measurements for tilt. A high quality temperature sensor can be included and a powerfull microprocessor (capable of 150 million multiplications each second) is calculating to produce results for real time output or storage to a logger e.g. SeaGuardII.

Figure 2-1 The Doppler Current Profiler Sensor 5400.

The configuration of tranducers on the DCPS is the so-called 'Janus' configuration, named after the Roman God, Janus, who could simultaneously look forward and backward. The configuration is particularly good for rejecting errors in horizontal velocity caused by instrument tilting since the two opposing beams allow vertical velocity components to cancel out when computing horizontal velocity. Also instrument tilting, pitch and roll cause velocity errors proportional to the sine of the pitch and roll. The four beams allow for calculation of two horizontal velocities with positive doppler shift (moving towards instrument) and two with negative (moving away) and four beams with vertical velocities. The direction of the vertical current is defined as positive when moving upwards.

Actually, horizontal current speed and direction can be calculated with just three beams. The fourth beam is redundant but in the DCPS it allows for an evaluation of whether the assumption of horizontal homogeneity (as described in **CHAPTER 3.1**) is reasonable, comparing the four vertical velocity estimates.

Utilizing four beams also makes it possible to calculate four different three-beam solutions by omitting one of the transducers. This can be useful in the case when for example one of the beams are receiving erroneous data caused by objects like mooring lines and floats that are not moving with the water flow. The DCPS has this ability built in (refer **CHAPTER 4.1**). It gives enhanced possibilities to understand the prevailing conditions and obtain high quality data.

The DCPS has two user selectable modes to measure currents; narrowband or broadband.

2.2 Narrowband Doppler Processing

The narrowband processing consists of measuring the frequency Doppler shift in order to calculate the current velocity and direction at different distance from the sensor. So far, we described the Doppler effect observer by one scatterer. When the transmitted signal is reflected from a number of scatterer distributed in the water volume, each of the scatterer will return an exact copy of the transmitted signal with a modified amplitude and phase (refer **Figure 2.2**). The phase of the signal will vary with the distance between the scatterer and the instrument and the amplitude of the reflected signal depends on the acoustic impedance of the scatterer, the size of the scatterer and the distance. Due to the random distribution of the scatterers both amplitude and phase will be more or less random. At the receiver all contributions of the distributed scatterers will be summed into a single signal. This summed signal will reflect the average Doppler shifted signal for this cell.

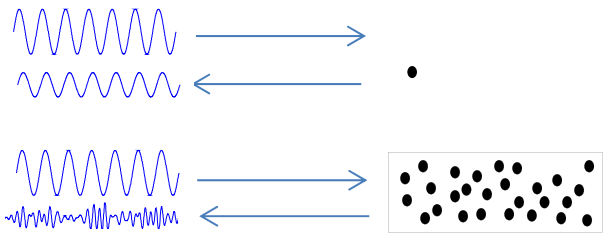

Figure 2-2. Reflection from a single reflector and cell containing a large number of scatterers

The DCPS working in the narrowband mode transmits pulses, which are pure sinusoidal signals with a fixed frequency of 600 kHz.

Depending on if the particles are moving away or toward the instrument the Doppler shifted signal will be a compressed or stretched versions of the transmitted signal.

2.3 Broadband Doppler Processing

A Doppler shifted signal will either be a compressed or stretched version of the original signal. The rate of compression can either be measured as a change of frequency (Narrowband processing), or estimated by measuring the change in pulse duration (Broadband processing). In broadband two identical pulses are transmitted as one transmission. The time delay between them are known at the transmitter and measured at the receiver. Based on the change in arrival time between the two pulses, the radial water current speed is calculated according to Eq.4.

The two pulses are designed in order to maximize the arrival time accuracy. A key feature to achieve this is to increase the bandwidth without shortening the pulse duration.

The accuracy of the time measurement for a given pulse is dependent on the bandwidth;

$$\Delta t \propto \frac{1}{BW}$$

By increasing the bandwidth, the uncertainty related to the time estimate will be reduced proportionally to the bandwidth. A bit simplified we could say that the bandwidth of a given signal will depend on the pulse duration and the change of frequency during the pulse duration. Shortening the pulse will increase the bandwidth, but the transmitted energy will also be reduced and shorter profiling ranges will be the result. Another better approach is to keep the pulse duration and at the same time increase the bandwidth. This can be achieved by using phase modulation or even better using frequency modulation. For a frequency modulated signal, the net frequency span during the transmission will give the bandwidth directly.

In narrowband the frequency is fixed, and the bandwidth of the pulse depends on the duration of the pulse. In Broadband mode, the DCPS transmits two successive identical sub-pulses in which the frequency gradually

sweep/chirp from 570 to 630 kHz with a known and fixed time lag in-between the two pulses (see **Figure 2-3**).

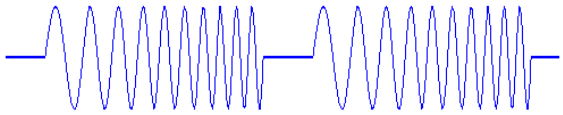

Figure 2-3: Illustration of a broadband Tx pulse, consisting of two identical pulses.

The bandwidth will then only depend on the frequency sweep, and be independent of the pulse duration (refer **Figure 2-4**). By measuring the time lag between the two pulses in reception, and comparing it to the pulse lag that was transmitted, the Doppler shift can be calculated.

Each of the sub pulses consists of a frequency chirp, i.e. the signal change frequency as a function of time.

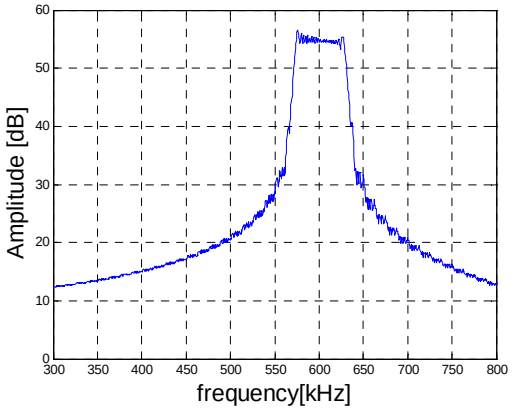

Figure 2-4: DCPS Tx pulse bandwidth.

In order to explain the principles of operation we will consider measurement at three different distances/cells along one of the four beams. The cells of interest are cell N and its two adjacent cells (see **Figure 2-5**).

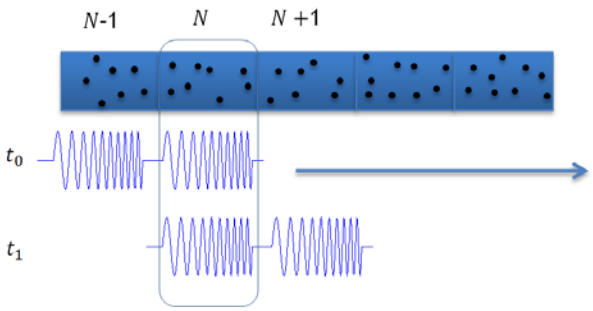

Figure 2-5: Illustration of a broadband Tx pulse, consisting of two identical sub pulses.

At time t_0, the transmitted pulse insonifies cell N and cell N-1. Particles moving in these two cells will reflect the signal back, and the received signal will be the sum of the reflections from these two cells. If the scatterers are uniformly distributed, 50% of the reflected signal will be from cell N and 50% will be from cell N-1.

Some milliseconds later at t_1, the transmitted signal has moved further and insonifies cell N+1 and N.

Because the two sub pulses are identical, the reflected signal from cell N at t_0 will be almost identical with the reflected signal from the same cell at t_1. By finding the maximum correlation between the two received signals from each cell the time lag between the two pulses can be measured. This time lag will be modified if the particles are moving towards the instrument or away from it. If the time between the two sub pulses at the transmitter is called T_0, and the change in lag from the reflected cell, compared to T_0 is called Δt, the Doppler shift and current speed v can be calculated with equation 4 below.

$$v = \frac{c}{2}\left(\frac{T_0}{T_0 + \Delta t} - 1\right) \qquad \textbf{Eq. 4}$$

Correlation factor:

By looking at **figure 2-5** we realize that the scatterer response from the first subpulse at t_0 will be identical to the last subpulse at t_1 if the scatterer remains the same at these two time instances. Likewise it will be sensible to assume that the response from the two remaining subpulses at t_0 and t_1 will be totally uncorrelated. If the scatterers are uniformly distributed, the scatterers stays within the cell and no noise is present, the correlation factor will be 0.5 reflecting a 50% correlation of the signal at t_0 and t_1. You could also argue that the signal is 100% for 50% of the pulse, whereas the remaining 50% of the pulse is totally uncorrelated.

There are three main effect that will modify the correlation factor.

1) The signal to noise ratio will gradually be reduced with range . This will in turn reduce the part of the signal that is correlated as the noise at t_0 and t_1 will be uncorrelated. With added noise the correlated part of the signal will no longer be 100% correlated.
2) If the scatterers are not uniformly distributed the energy in the correlated part will no longer represent 50% of the total reflected energy. This will be the case when the signal hits an object or a boundary like the surface or bottom. The correlation factor will typically follow these transitions low-high-low when an object is reflecting the transmitted pulses.
3) In order for the correlated part to be 100% it will require the scatterers to remain identical for the time duration t_1-t_0. This can only be achieved in the case of 0 water current and the scatterers remains stationary. When the scatterers are exposed to current, some of the scatterers will move out of the cell, and some new scatterers will move in. Due to the short time duration t_1-t_0, the scatterers experience very little movement, and the correlation factor for high SNR (Signal to Noise Ratio) cells are close to 0.5.

Ambiguity:

The output of the correlation process is a phase value. When the Doppler shift is zero the phase is zero. When the Doppler shifts increase, so will the phase. A Doppler shift of approximately 1.25 m/s along the beam corresponds to a phase equal to 360 (360 = 0) which is exactly the same as for zero Doppler shift. For this reason the cross correlation process is not able to distinguish a Doppler shift of 1.5 from a Dopler shift of zero. In fact any Doppler shift outside the 1.25m/s range will be wrongly detected to be within the range 0 – 1.25 m/s.

This is called ambiguity and could hamper the correct operation of the instrument if not corrected for.

For a DCPS sensor in broadband mode, the centre frequency is 600 kHz. One period of average frequency of 600 kHz corresponds to a period time of $T_0 = 1.67 \cdot 10^{-6} s$. By using Eq. 4 the ambiguity Doppler speed along the beam is calculated to be 1.25m/s.

Taking into account the orientation of the beams, θ=25 degrees off the vertical axis, the corresponding ambiguity horizontal speed will be:

$$v_{hor} = \frac{v_{beam}}{\sin(\theta)} = \mp 1.48 m/s$$

By allowing some tilt, a useful unambiguous speed of at least 1m/s will be achieved. The ambiguity lock function of the DCPS broadband mode can be used in order to lock the

instrument in a horizontal current range, which is below 1m/s.

If the user is confident that the horizontal current will not exceed 1 m/s this configuration would be the preferred broadband configuration.

In case the ambiguity lock is not selected, several stages of ambiguity solving methods are automatically implemented in the DCPS in order to achieve a non-ambiguous solution.

These methods include:

- Use of transmission pulses that are designed to give different ambiguity intervals. The combination of phase output from these set of pulses are unique for a limited number of intervals.
- Remaining ambiguities are solved by putting consistency requirement on neighbouring cells in time and space and using statistics in order to resolve potential ambiguity.

Compared to *Narrowband,* the *Broadband* mode gives a reduction in single ping standard deviation of a factor four to five.

Consequently fewer pulses can be used to obtain high quality current data, which reduces the power consumption of the sensor, by almost the same factor.

Limitation in the automatic ambiguity solution:

The ambiguity resolving method incorporates use of two different Tx pulse sets each consisting of two sub pulses. In order to be able to resolve the ambiguity correctly, the 3D water current vector, as seen from the instrument should be fairly equal for two successive transmissions. If the instrument is exposed to movement during the measurement phase, this requirement would be violated and increase the probability of having unfiltered ambiguities in the detected current measurements.

This could be the case if the instrument is installed on a surface platform exposed to heavy seas. Normal current fluctuations do not cause any problem to the ambiguity resolution algorithm.

If horizontal current speed is expected to be above 1m/s and the instrument is expected to move around rapidly, narrowband mode is the preferred mode to be used.

2.4 From signal transmission to reception

Whether the instrument is configured in broadband or narrowband, the user needs to configure the number of cells and the cell size (from 0,5 to 5m).

The cell could be defined as the volume of water in which the instrument is performing the measurement.

By defining the cell size and the number of cells, and knowing the speed of sound, the instrument determines the time frame when the reflected signal from the corresponding cell will be received.

In the **Figure 2-6**, at t0, the sensors transmits the acoustic pulse. At the receiver the recording for the first cell (C0) starts when the center of the transmitted pulse reaches the beginning of C0 at t2, and stops when the center of the pulse leaves C0 at t4. In other words, the receiver collects samples for the same duration as the transmitted pulse. In Narrowband, the extent of the pulse in water also matches the cell size.

IIt will corresponds to t1, when it reaches the second cell (cell1), it will correspond to t2, etc. The blanking zone is defined as the time needed for the transducer to shift from transmitting mode to receiving mode. For this

reason the receiver will always start the measurement outside the blanking zone. The blanking zone is equivalent to 1 meter.

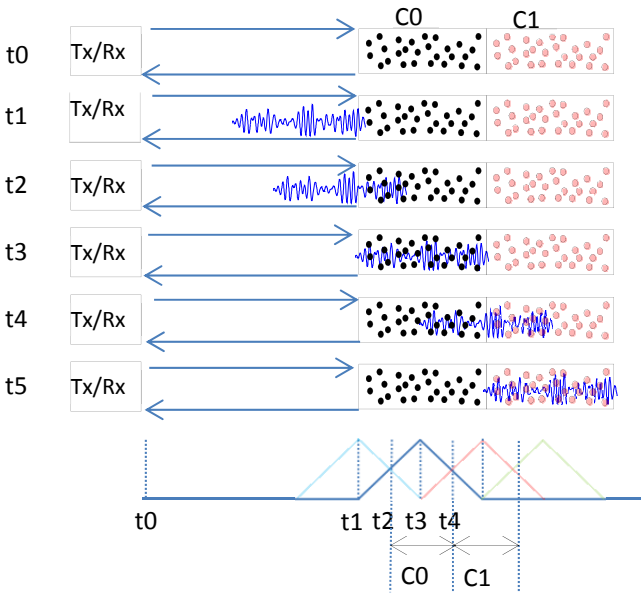

Figure 2-6: Transmission/Reception of reflected signal

Overlap function:

When configuring the instrument, it is possible to define a cell overlap from 10% to 90%. When no overlap is selected, the samples that defines each cell is only used in this particular cell. If the instrument is set up with overlap, the size of the cell is not changed, but the spacing between them is reduced as the next cell will "overlap" the previous cell.

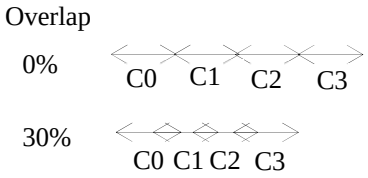

Figure 2-7: Principles of overlap

In the **Figure 2-7** the cell spacing is indicated by the spacing of the arrow and the cell size is indicated by the length of the arrow. In this example 30% overlap is selected. That means that 30% of the samples for C0/C1 is common and 30% of the samples for C1/C2 is common and so on.

The advantage by using overlap is that one can reduce the cell spacing without reducing the cell size. This feature is especially useful when it is important to measure the current as close to the surface/bottom as possible. Cells that contains samples from the surface/bottom are contaminated by the strong surface/bottom reflections and are not usable for measuring the current. By having small spacing between cells the last good uncontaminated cell can easily be picked out. It will also improve the vertical resolution without reducing the cell size.

Multiple columns - surface or instrument reference functions :

When configuring the instrument it is possible to define up to three columns (profiles) simultaneously for optimum flexibility.
Each column may be set-up with individual cell size and cell overlap, and may further be defined as being either instrument referred or surface referred (requires pressure sensor).
When a column is instrument referred, the distance from the instrument to the start of the column is kept constant; a setting which is usually used in deep waters where the surface is distant or when bottom currents are to be monitored. Refer **Figure 2-8**.

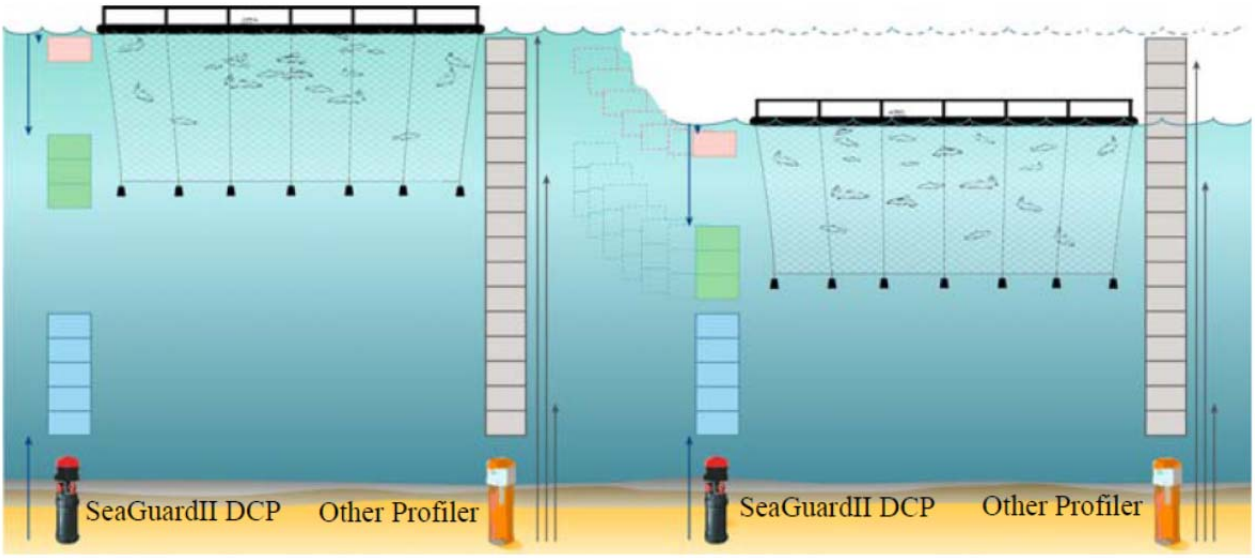

Figure 2-8: Illustration of the multiple columns capability and surface or instrument referred

CHAPTER 3 Calculation of vertical and horizontal currents

3.1 Obtaining currents from multiple levels above/below the sensor

The four transducers transmit short pulses (pings) of acoustic energy into the water which are reflected against particles. By systematically clocking these reflections further and further away from the sensor and collecting their doppler shift, currents can be measured at multiple levels, up to 150 (divided over three columns; column 1: max 75 cells, column 2; max 50 cells and column 3 with 25 cells) simultaneously. For more information refer to the DCPS manual TD304).

An important factor in this context is knowing the speed of sound at the sensor which is obtained from an intergrated temperature sensor and assumed or measured salinity and pressure information. All instruments from Aanderaa have the option for plug-and play addition of smart-sensors for salinity, pressure and other parameters. It is possible to calculate the speed of sound "dynamically" so the sensor sends speed of sound changes based on values obtained from the sensors "continuously" to the DCPS sensor.

In most cases for a sensor like the DCPS that has a maximum range of about 100 m in the best case, it is not important to know the full sound speed profile above/below. A strong stratification with large differences in sound speed could however have implications for at what distance from the instrument the cells are located.

The DCPS sensor is operating at around 600 kHz which gives a typical range of 40-100 m depending on the scatter conditions. In general clear water with a low amount of particles gives shorter range and so do warm water. But also in situations where there is too much particles in the water (above 100 mg/l), like in a turbid river the range will be limited.

For the Doppler current technique to be valid, some assumptions must be fulfilled:

1. The scatterers must drift with the water currents.

2. The water motions must be of a large scale compared to the separation of the beams (horizontal homogenity of the water).

3. The water motions must be of a large scale compared to the length of the transmitted pulse (vertical homogenity of the water).

The first assumption is critical since the movement of the scatterers in the water volume represents the water movement. It is essential that the scatterers do not move by themselves differently from the water current.

The other two assumtions are less critical.

3.1.1 Relationship between current measured at beams and earth referenced current.

The DCPS has four transducers that are oriented 90° in azimuth to each other and with a 25° angle to the vertical. The transmitted signal from the transducers 1 to 4 will propagate in the pointing directions of the transducers and are denoted Beam1 – Beam4 (Refer **Figure 3-1**). In the sensors reference system (x, y, z) the pointing directions for the transducers are defined as follows;

- Beam 1. Pointing in positive x-axis and positive z-axis direction (x_1=sin(θ), y_1=0, z_1=cos (θ)).
- Beam 2. Pointing in negative y-axis and positive z-axis direction (x_2=0, y_2= -sin(θ), z_2=cos (θ)).

- Beam 3. Pointing in negative x-axis and positive z-axis direction (x_3=-sin (θ), y_3=0, z_3=cos (θ)).
- Beam 4. Pointing in positive y-axis and positive z-axis direction (x_4=0, y_4= sin (θ), z_4=cos (θ)).

The sensor reference system is defined by a right handed system with x-axis aligned with north axis, y-axis aligned with west and z-axis aligned with up if pitch, roll and heading are all zero.

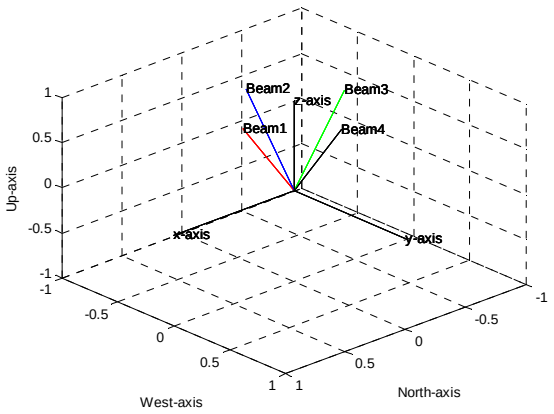

Figure 3-1. Sensor/beam geometry.

<u>Decomposition of current Doppler vector along beams:</u>

A positive Doppler shift is measured when the current is going towards the transducer. Any current direction can be decomposed into the sensors x, y and z axis. In case of a current parallel to the x-axis, only beam1 and beam3 will be able to measure the current, and similarly for a current parallel to the y-axis only the beam2 and beam4 will be able to measure the current. In these two special cases the current will be orthogonal to the two remaining beams, hence no current will be measured at these beams.

For each of the current directions x, y, and z, the contribution from each of the sensors will be reduced due to the angle between each of the beams and the x,y and z axis. (refer **Figure 3-2.**)

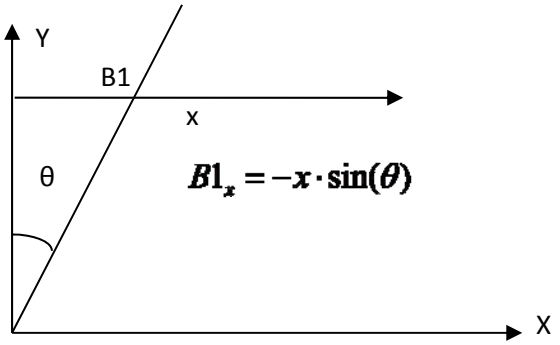

Figure 3-2: decomposition of beam currents

Correspondingly if the current is described in the sensors reference frame x, y and z each of the beam currents can be described. The following equations gives the relationship between the decomposed current field (x,y,z) and the contribution on each of the sensors.

$$B1_x = -x \cdot \sin(\theta),\ B2_x = 0,\ B3_x = x \cdot \sin(\theta),\ B4_x = 0$$

$$B1_y = 0,\ B2_y = y \cdot \sin(\theta),\ B3_y = 0,\ B4_y = -y \cdot \sin(\theta)$$

$$B1_z = -z \cdot \cos(\theta),\ B2_z = -z \cdot \cos(\theta),\ B3_z = -z \cdot \cos(\theta), B4_z = -z \cdot \cos(\theta)$$

By summing the contribution from each of the sensors for the axis x, y and z, the following equations can be derived.

$$B3_x - B1_x = 2x \cdot \cos(\theta) \quad \Rightarrow x = \frac{1}{2\sin(\theta)}(S3_x - S1_x) \qquad (1)$$

$$B2_y - B4_y = 2y \cdot \sin(\theta) \quad \Rightarrow y = \frac{1}{2\sin(\theta)}(S2_y - S4_y) \qquad (2)$$

$$B1_z + B2_z + B3_z + B3_z = -4z \cdot \cos(\theta) \Rightarrow z = -\frac{1}{4\cos(\theta)}(B1_z + B2_z + B3_z + B4_z) \qquad (3)$$

The equations (1-3) gives the relationship between the beam current and the decomposed current x, y and z.

3.1.2 Transformation from the instrument reference system to the earth reference system

The build in accelerometer and magnetometer is used to establish the orientation of the instrument relative to the earth reference system. The output from the "orientation

sensor" is described as a rotation of the sensor along each of the axis x, y, and z. As mentioned earlier, for a non-rotated sensor, the x-axis will be aligned with north, the y-axis will be aligned with west, and the z-axis will be aligned with up. A positive rotation around the x-axis corresponds to a positive roll value. A positive rotation around the y-axis corresponds to a negative pitch value, and finally a positive rotation around the z-axis corresponds to a negative value (counter clock rotation).

Each of these rotations can be described by a rotation matrix:

$$\begin{bmatrix} x' \\ y' \\ z' \end{bmatrix} = \begin{bmatrix} 1 & 0 & 0 \\ 0 & \cos(\theta) & -\sin(\theta) \\ 0 & \sin(\theta) & \cos(\theta) \end{bmatrix} \begin{bmatrix} x \\ y \\ z \end{bmatrix} \qquad \mathbf{u}_x = \mathbf{A}_x \cdot \mathbf{u} \qquad \theta : x-axis\ rotation$$

$$\begin{bmatrix} x' \\ y' \\ z' \end{bmatrix} = \begin{bmatrix} \cos(\varphi) & 0 & \sin(\varphi) \\ 0 & 1 & 0 \\ -\sin(\varphi) & 0 & \cos(\varphi) \end{bmatrix} \begin{bmatrix} x \\ y \\ z \end{bmatrix} \qquad \mathbf{u}_y = \mathbf{B}_y \cdot \mathbf{u} \qquad \varphi : y-axis\ rotation$$

$$\begin{bmatrix} x' \\ y' \\ z' \end{bmatrix} = \begin{bmatrix} \cos(\phi) & -\sin(\phi) & 0 \\ \sin(\phi) & \cos(\phi) & 0 \\ 0 & 0 & 1 \end{bmatrix} \begin{bmatrix} x \\ y \\ z \end{bmatrix} \qquad \mathbf{u}_z = \mathbf{C}_z \cdot \mathbf{u} \qquad \phi : z-axis\ rotation$$

By multiplying the rotation matrixes, the combined total rotation matrix can be found:

$$\mathbf{u}_{Earth} = \mathbf{C}_z \cdot \mathbf{B}_y \cdot \mathbf{A}_x \cdot \mathbf{u} = \mathbf{D}_{xyz} \cdot \mathbf{u}$$

When $\mathbf{u}$ is related to the current in the sensor reference frame (x,y,z), the $\mathbf{u}_{Earth}$ will be related to the current in the earth reference frame. The product $\mathbf{D} = \mathbf{C}_z \cdot \mathbf{B}_y \cdot \mathbf{A}_x$ can be expressed by:

$$\mathbf{D} = \begin{bmatrix} \cos(\phi)\cos(\varphi) & \cos(\phi)\sin(\varphi)\sin(\theta) - \sin(\phi)\cos(\theta) & \cos(\phi)\sin(\varphi)\cos(\theta) + \sin(\phi)\sin(\theta) \\ \sin(\phi)\cos(\varphi) & \sin(\phi)\sin(\varphi)\sin(\theta) + \cos(\phi)\cos(\theta) & \sin(\phi)\sin(\varphi)\cos(\theta) - \cos(\phi)\sin(\theta) \\ -\sin(\varphi) & \cos(\varphi)\sin(\theta) & \cos(\varphi)\cos(\theta) \end{bmatrix}$$

This gives the relationship between the current in sensor reference frame and the current in earth reference frame.

$$north = x \cdot \cos(\phi)\cos(\varphi) + y \cdot (\cos(\phi)\sin(\varphi)\sin(\theta) - \sin(\phi)\cos(\theta)) + z \cdot (\cos(\phi)\sin(\varphi)\cos(\theta) + \sin(\phi)\sin(\theta)) \quad (4)$$

$$west = x \cdot \sin(\phi)\cos(\varphi) + y \cdot (\sin(\phi)\sin(\varphi)\sin(\theta) + \cos(\phi)\cos(\theta)) + z \cdot (\sin(\phi)\sin(\varphi)\cos(\theta) - \cos(\phi)\sin(\theta)) \quad (5)$$

$$up = -x \cdot \sin(\theta) + y \cdot (\cos(\varphi)\sin(\theta)) + z \cdot (\cos(\varphi)\cos(\theta)) \quad (6)$$

The combination of equation (1-3) and (4-6) gives the necessary equations in order to convert Doppler current measurement from the four beams into the current given in the earth coordinate reference frame for a given orientation of the sensor. The sensor orientation is measured for each ping. Within a record the current are averaged in the earth reference frame while utilizing the orientation measurement individually on a ping to ping basis.

At each depth level and for each of the four beams the total Doppler shift is obtained. To this both vertical and horizontal currents contribute but the contribution from the horizontal currents is normally larger because these currents are typically about 10 times stronger (unless there is strong up/down welling).

By using the descrived trigonometry, the current speed obtained from the Doppler shift given by each transducers is decomposed into positive or negative (moving towards or away from the transducer) currents in the X, Y and Z planes. By summing these up from the different beams and correcting for how the instrument was oriented with input from the compass and the accelerometer the speed and direction is calculated. After this calculation is done an adjustment for sound speed, fixed or measured, is implemented.

A minimum of 3 beams is needed to do these calculations but the DCPS has 4. In the DCPS the beams redundancy gives the possibility to calculate four 3-beam solutions and compare these with each other and with the 4-beam calculation. This is particularly useful if there are disturbing objects in one of the beams or if the circulation pattern is heterogeneous (described in **Chapter 4-1**).

3.2 Compensation for tilt and rotation in each measurement (ping)

With the inbuilt 3-axes compass (gives heading) and an accelerometer (gives tilt) each single is compensated for tilt and rotation of the sensor.

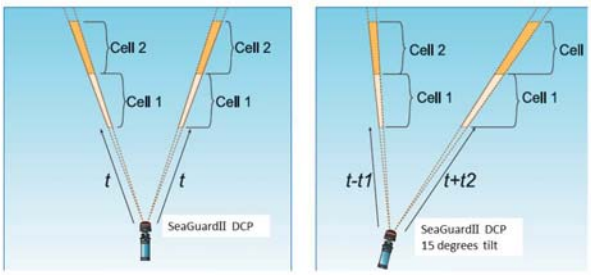

Figure 3-2: Illustration of the beam repositioning when the instrument is tilted; example with 15 degrees tilt

Beam repositioning: refer Figure 3-2
When the sensor is tilting in one direction two of the beams will become more horizontally oriented and two more vertically oriented. The more vertically oriented beams will have a shorter travelling distance than the more horizontally oriented beams to reach the depth level / the cell at which the current will be measured. The DCPS is automatically tilt/time compensate the individual beams for each measurement so that the Doppler shift obtained for all the four beams will be obtained from the same depth level. The advantage of this technology is not only that the true horizontal layer is monitored, it also prevents an increase in the side lobe caused illegible zone close to the surface when the instrument is tilted. The tilt compensation algorithm is updated for each ping and works with tilts up to ±50°. Above ±35°, the tilt sensor is outside the calibrated range. The profiling range and accuracy will decrease. For indication, at 50° tilt, the effective range will be 25m.

3.3 Surface current measurements

The DCPS, when upward looking, has the unique ability to measure surface currents in the top cm layer (it requires pressure data either using a pressure/tide/wave sensor sending data to the DCPS or mounted on the SeaGuardII equipped with pressure/tide/wave sensor). When it comes to the surface cell, the impedance difference between the water and air creates an almost perfect reflector. The backscattered energy from the surface is normally extremely strong compared to the reflections from particles in the water and will totally dominate this cell. The pressure/wave/tide sensor is needed to determine when the strongest part of the reflection will be returned to the instrument and then the Doppler Shift for this reflection is calculated.

Due to the strong reflection from the surface boundary layer it is possible to detect the surface cell at longer range (100 m) compared to ordinary cells.
The surface cell will reflect the speed of the “boundary condition”. Wind will generate capillary waves, and rapidly accelerate the surface boundary. For this reason there will be a strong correlation between both wind speed/surface boundary speed and wind direction / surface boundary direction.

CHAPTER 4 The DCPS produces high quality data

4.1 Innovative three beam solution

The DCPS is equipped with unique software that makes it possible to obtain high quality current data even if one of the four beams is disturbed by for example an object. This can be useful in the case when for example one of the beams are receiving erroneous data caused by objects like mooring lines and floats that are not moving with the water flow. The DCPS has this ability built in. It gives enhanced possibilities to understand the prevailing conditions and obtain high quality data.

There are several ways to control the quality of the measurements. These are described in detail in the DCPS manual TD304. Quality parameters include Acoustic Signal Strength (low signal indicate limit of reach), Standard Deviation of the current speed (high standard deviation can be caused by mixing/turbulence and when the signal strength is weak) and Cross Difference (for each depth the speed in beam 1 - speed beam 3 + speed beam 2 – speed beam 4 should be close to 0).

If the quality parameters indicate that the four beam solution are not consistent, perhaps due to an obstruction in one of the beams, the *Auto Beam solution* will use the three beam solution with the lowest single ping standard deviation to calculate the current speed. If the *Cross Difference* parameter indicates that the four-beam solution is consistent and of good quality, the *Four*-Beam solution will automatically be selected as the preferred *Auto Beam* solution. Thus, the four-beam solution is selected unless the *Cross Difference* of this solution is above a certain threshold.

The operator can choose to activate output for all beam solutions, *Auto Beam*, *Four Beam* and the four *Three Beam* solutions. This gives enhanced possibilities of quality control.

Using the trigonometry described in the **Chapter 3-1,** it is possible to derive the equations for the three beam solutions as listed in the table:

	Beam 1,2,3	Beam 1,2,4	Beam 1,3,4	Beam 2,3,4
x	$\frac{(B3-B1)}{2\cdot\sin(\theta)}$	$\frac{((B2+B4)/2-B1)}{\sin(\theta)}$	$\frac{(B3-B1)}{2\cdot\sin(\theta)}$	$\frac{(B3-(B2+B4)/2))}{\sin(\theta)}$
y	$\frac{(B2-(B1+B3)/2)}{\sin(\theta)}$	$\frac{(B2-B4)}{2\cdot\sin(\theta)}$	$\frac{((B1+B3)/2-B4)}{\sin(\theta)}$	$\frac{(B2-B4)}{2\cdot\sin(\theta)}$
z	$\frac{(B1+B3)}{-2\cdot\cos(\theta)}$	$\frac{(B2+B4)}{-2\cdot\cos(\theta)}$	$\frac{(B1+B3)}{-2\cdot\cos(\theta)}$	$\frac{(B2+B4)}{-2\cdot\cos(\theta)}$

4.2 Calculating the noise levels/standard deviation

Depending on the mode, the DCPS transmits either a single tone burst or a broadband coded signal of duration T_p (refer **CHAPTER 2** – Broadband principles of operation). The returned signal is compared to the transmitted pulse at a fixed time lag T_L (correlation).

The weaker the correlation the noisier the data, which means less precision in the velocity estimate.

The standard deviation, σ, of an ensemble of pings is:

$$\sigma = \frac{A}{f_S\sqrt{D\cdot P_L}}\frac{1}{\sqrt{N_p}} \qquad \textbf{Eq. 5}$$

where N_p is the number of pings, D is the cell size and P_L is the pulselength. In narrowband, the pulselength is set equal to the cell size, whereas in broadband the pulselength is fixed. The constant, A, is dependent on the mode (broadband/narrowband), frequency, bandwidth, SNR (signal-to-noise ratio) and other properties related to the signal processing.

4.3 DCPS Narrowband internal processing –ARMA model

In Narrowband mode, the DCPS uses an Auto Regressive Moving Average (ARMA) model to estimate spectral properties of the backscattered signal.

The ARMA spectral estimation technique belongs to a family of spectral estimators called parametric models.

The motivation for using parametric models is the ability to achieve better power spectrum estimation than that produced by classical spectral estimators.

CHAPTER 5 Limitations of Doppler Current Profilers

Physical and technical limitations of a Doppler Current Profiler are:

- Precision in the estimation of the Doppler frequency.
- Influence of acoustic side lobes.
- Measurement range.
- Blanking distance.
- Random and systematic errors.

The precision in the estimation of the Doppler frequency has been discussed previously. The other limitations are discussed in this chapter.

5.1 Influence of acoustic side lobes and the contaminated zone close to surface/bottom

Typically, the beam pattern of an acoustic transducer has one main lobe and a number of lower energy side lobes on both sides of the main lobe. A theoretical beam pattern (-30° to +30°) for a plane circular piston is given in **Figure 5-1** , for illustration.

The main lobe is centred around 0°, the first set of side lobes are seen at approximately ±15° and the second set of side lobes at approximately ±25°. The level of the maximum signal in the first side lobe is approximately 17 dB lower than the maximum signal in the main lobe.

The DCPS transducers are tilted 25° off the vertical axis. Hence, the distance to the surface/bottom along the vertical axis is shorter than along the main lobe axis.

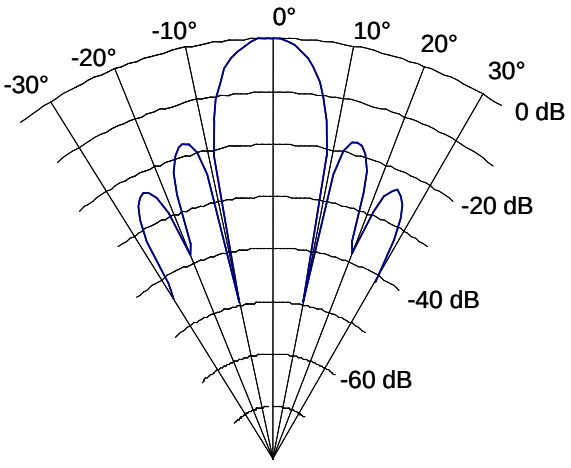

Figure 5-1: Beam pattern

As a result, strong signals backscattered off the surface/bottom originating from the side lobes that arrive at the same time as the backscattered signal from the main lobe will "acoustically contaminate" measurements close to boundaries like the surface (upward looking)

and the bottom (downward looking). Typically the contaminated zone is about 10 % of the deployment depth (when upward looking) or water depth (if instrument is downward looking). Please observe that surface current measurements, described in **chapter 3-3**, are not affected by the side lobe contamination.

An illustration of the 'good range', *R*, and obscure range near the surface is given in **Figure 5-2.**

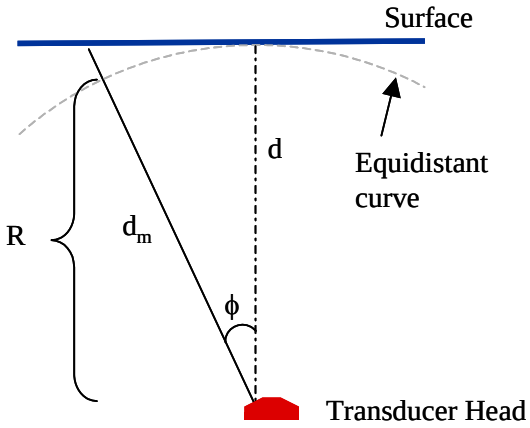

Figure 5-2: Illustration of the good measurement range, R.

Here, the distance to the surface along the vertical axis is denoted *d* and the distance along the main lobe axis is denoted d_m. The blue solid line indicates the surface, and the grey dotted curve indicates the equidistant curve from the transducer.

The cells at a distance from the transducer greater than *R* may be obscure, while the cells at a distance from the transducer smaller than *R* are inside a good measurement range.

The expected good range is stated as

$$R = d \cdot \cos(\phi) \qquad \textbf{Eq. 6}$$

where *d* is the vertical distance from the transducers to the surface and ϕ is the beam angle relative to the vertical. Thus, for a 25° beam angle about 10% of the water volume closest to the surface may hold inaccurate data.

5.2 Total measurement range

The total measurement range depends on the source level i.e. the transmitted power, the transducer efficiency and the frequency. At 600 kHz, the transducers are relatively small and their efficiency is limited by non-linear behaviour and cavitation. Hence for linear wave propagation, the transmitted power of a small transducer is limited. An increased pulse length may increase the range by a small amount.

Field data has demonstrated that the DCPS has an approximate range of 40-100 m depending on the scattering conditions. The range is similar using broadband and narrowband.

5.3 Blanking distance closest to the instrument

After transmitting an acoustic pulse, the transducers and electronics must rest a short time for the transducers to stop vibrating (ringing) before it is able to act as a microphone and receive the very weak (compared to the transmitted pulse) reflected acoustic signals.

The ringing of the transducers depends on transducer size, frequency and the material embedding the transducers.

About half a millisecond of ringing corresponds to a 1 m blanking distance assuming a sound speed in water of 1500 m/s.

5.4 Random and systematic errors

Two types of errors contribute to velocity uncertainty; random and systematic (bias) errors. Random errors can be averaged out while systematic errors cannot.

Random errors are reduced by the square root of the number of samples in one record.

Random errors depend on a number of factors:

- Pulse Length: The shorter the pulse length, the greater the random error for a given frequency.
- Transmit Frequency: The lower the frequency, the greater the random error for a given pulse length.

- SNR: The lower the signal-to-noise ratio, the greater the random error.

Bias errors are non-random and can therefore not be reduced by data averaging. Fortunately, these errors are in general small, typically ~0.5 cm/s. The expression for the standard deviation is already shown in **Eq. 5**.

5.4.1 Beam separation

The separation of the 4 transducer beams poses a limit to the vertical and horizontal scales of motion that can be resolved. With increasing distance from the transducer the sampling volume (cell volume) and the distance between the 4 cells at the same distance from the transducer increase. Thus, a short period velocity fluctuation resolved in close range may not be resolved in the end of range where the horizontal distance between the cells is greater.

5.4.2 Echo intensity and backscatters

A 600 kHz transducer transmits sound waves with a wavelength of a couple of millimetres. These waves may bounce off small planktons, particles or air-bubbles that have an acoustic impedance difference to the medium itself; the water. Bubbles, however, are compressible and take energy from the sound waves and thus often limit the range. Bubble clouds exist e.g. in the surface wave break zone or in the wake of ships.

In oceanographic applications the main limitation for obtaining good data at a distance from the sensor is poor backscatter. If the scatterers are comprised of large zooplankton moving independently of the water current, a very critical *assumption* is violated and data may be obscured.

If the scatterers are too few the backscattered energy is low and self-noise may corrupt the signal. The backscattered energy, or the *Echo Intensity,* is measured by the instrument relative to the maximum intensity.

Echo intensity can be used not only as a quality parameter but also to record temporal and spatial relative abundance of plankton, particles and/or bubbles. The Sonar equation has to be employed and biological 'ground proof' needs to be taken.

An estimate of the relative backscatter, R_B *[dBm^{-1}]*, can be calculated as:

$$R_B = EI - 20\log_{10}(d_s) - 2\cdot\alpha\cdot d_s \quad \textbf{Eq. 7}$$

where *EI* is the echo intensity, d_s is the distance to the scatterers along the beam, and α is the sound absorption.

The other two terms in the equation are the volume attenuation by beam spreading, $20\log_{10}(d_s)$ and a decay of the signal due to sound absorption, $2\cdot\alpha\cdot d_s$.

To calculate absolute backscatter several factors like

- Signal power
- Noise level
- Transducer efficiency
- Effective diameter

have to be included.

Beam Spreading:

Beam spreading is a geometric cause for echo attenuation as a function of range. It can be found that inside the DCPS measurement range the amplitude is inversely proportional to the distance squared, i.e. $\sim\frac{1}{d_T{}^2}$ (in linear units) where d_T is the distance from the transducers.

The decay in amplitude may be understood as the result of the transducers intersecting only a fraction of the reflected energy.

Sound absorption:

Absorption involves a process of conversion of acoustic energy to heat and thereby represents a true loss of energy to the medium in which propagation is taking place.

An often used model for calculation of the absorption, α, is the Francois-Garrison model which is a refinement of the Fisher-Simmons model. The Francois-Garrison model is valid in low temperature environments.

References

- Francois, R.E., Garrison, G.R., 1982. Sound absorption based on ocean measurements. Part II: Boric acid contribution and equation for total absorption. J. Acoust. Soc. Am. 72 1879-1890
- Simpson, M.R., 2001, Discharge measurements using a broadband acoustic Doppler current profiler. United States Geological Survey, Open-file-report 01-1
- Urick, R.J., 1983, Principles of underwater sound. (3rd edition): McGraw-Hill, San Francisco, USA
- Kinsler & Frey, Fundamentals of Acoustics. (3rd edition): John Wiley & Sons
- François Le Chevalier, Principles of Radar and Sonar Signal Processing, Artech House Publishers
- Almroth-Rosell E., A. Tengberg, S. Andersson, A. Apler and P.O.J. Hall (2012). Effects of simulated natural and massive resuspension on benthic oxygen, nutrient and dissolved inorgani c carbon fluxes in Loch Creran, Scotland. *Journal of Sea Research*, **72**, 38-48.
- Atamanchuk D., M. Kononets, P.J. Thomas, J. Hovdenes, A. Tengberg and P.O.J. Hall (2015) Continuous lo ng-term observations of the carbonate system dynamics in the water column of a temperate fjord. *Journal of Marine Systems*, **148**, 272–284.
- Francis O.P. and D. E. Atkinson (2012) Synoptic forcing of wave states in the southeast Chukchi Sea, Alaska, at nearshore locations . *Natural Hazards*, **62**: 1273–1300.
- Francis O.P. and D. E. Atkinson (2012) Synoptic forcing of wave states in the southeast Chukchi Sea, Alaska, at an offshore location. *Natural Hazards*, **62**: 1169–1189.
- Francis O.P., G.G. Panteleev and D. E. Atkinson(2011) Ocean wave conditions in the Chukchi Sea from satellite and in situ observations. *Geophysical Research Letters*, **38**, L24610, doi:10.1029/2011GL049839.
- Friedrich J., F. Janssen, D. Aleynik, H.W. Bange, N. Boltacheva, M.N. Çağatay, A.W. Dale, G. Etiope, Z. Erde m, M. Geraga, A. Gilli, M.T. Gomoiu, P.O.J. Hall, D. Hansson, Y. He, M. Holtappels, M. K. Kirf, M. Kononets, S. Konovalov, A. Lichtschlag, D. M. Livingstone, G. Marinaro, S. Mazlumyan, S. Naeher, 17, R.P. North, G. Papatheodorou, O. Pfannkuche, R. Prien, G. Rehder, C.J. Schubert, T. Soltwedel, S. Sommer, H. Stahl, E. V . Stanev, A. Teaca, A. Tengberg, C. Waldmann, B. Wehrli and F. Wenzhöfer (2014). Investigating hypoxia in aquatic environments: diverse approaches to addressing a complex phenomenon . *Biogeosciences*, **11**, 1215–1259.
- Oguri K., Y. Furushima, T. Toyofuku, T. Kasaya, M. Wakita, S. Watanabe, K. Fujikura, H. Kitazato (2015). Long-term monitoring of bottom environments of the continental slope off Otsuchi Bay, northeastern Japan . *Journal of Oceanography*, Special Issue Oceanographic Observations After The 2011 Earthquake Off The Pacific Coast Of Tohoku, pp 1-16.
- Suursaar U. (2010) Waves, currents and sea level variations along the Letipea – Sillamae coastal section of the southern Gulf of Finland. *Oceanologia,* **52 (3)**, 391–416.
- Suursaar U. and R. Aps (2007) Spatio-temporal variations in hydro-physical and -chemical parameters during a major upwelling event off the southern coast of the Gulf of Finland in summer 2006. *Oceanologia*, **49 (2)**, 209–228.
- Suursaar U, J. Jaagus, A. Kontc, R. Rivis, H. Tonisson (2008) Field observations on hydrodynamic and coastal geomorphic processes

off Harilaid Peninsula (Baltic Sea) in winter and spring 2006–2007. *Estuarine, Coastal and Shelf Science*, **80**, 31–41.

- Suursaar U., T. Kullas and R. Aps (2012) Currents and waves in the northern Gulf of Riga: measurement and long-term hindcast. *Oceanologia,* **54 (3)**, 421–447.

- Tengberg A., E. Almroth and P.O.J. Hall (2003). Resuspension and its effect on organic carbon recycling an d nutrient exchange in coastal sediments: In-situ measurements using new experimental technology. *Journal of Experimental Marine Biology and Ecol ogy*, **285-286**: 119-142.

- Wesslander K., P. Hall, S. Hjalmarsson, D. Lefevre, A. Omstedt, A. Rutgersson, E. Sahlée and A. Tengberg (2011) Observed carbon dioxide and oxygen dynamics in a Baltic Sea coastal region. *Journal of Marine Syst ems*, **86**: 1–9.

Aanderaa Data Instruments AS
P.O.Box 103 Midtun, Sanddalsringen 5b, N-5828 Bergen, Norway
Tel: +47 55 60 48 00 Fax: +47 55 60 48 01
email: aanderaa.info@xyleminc.com - www.aanderaa.com

xylem
Let's Solve Water